

Topical administration of GLP-1 eyedrops improves retinal ganglion cell function by facilitating presynaptic GABA release in early experimental diabetes

Yu-Qi Shao, Yong-Chen Wang, Lu Wang, Hang-Ze Ruan, Yun-Feng Liu, Ti-Hui Zhang, Shi-Jun Weng, Xiong-Li Yang, Yong-Mei Zhong*

<https://doi.org/10.4103/NRR.NRR-D-24-00001>

Date of submission: January 1, 2024

Date of decision: March 9, 2024

Date of acceptance: April 12, 2024

Date of web publication: June 26, 2024

From the Contents

Introduction

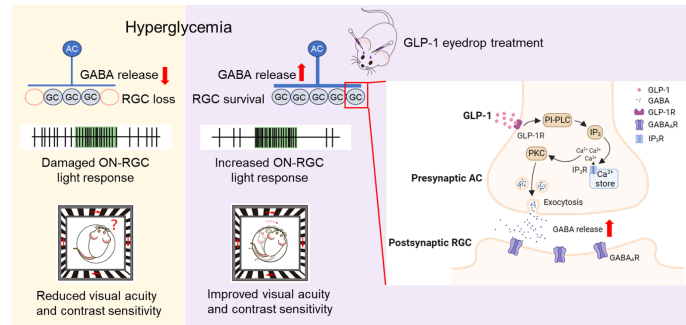
Methods

Results

Discussion

Graphical Abstract

Treatment with GLP-1 eyedrops protects damaged retinal ganglion cells and improves visual impairment by modulating presynaptic GABA release in early diabetes



Abstract

Diabetic retinopathy is a prominent cause of blindness in adults, with early retinal ganglion cell loss contributing to visual dysfunction or blindness. In the brain, defects in γ -aminobutyric acid synaptic transmission are associated with pathophysiological and neurodegenerative disorders, whereas glucagon-like peptide-1 has demonstrated neuroprotective effects. However, it is not yet clear whether diabetes causes alterations in inhibitory input to retinal ganglion cells and whether and how glucagon-like peptide-1 protects against neurodegeneration in the diabetic retina through regulating inhibitory synaptic transmission to retinal ganglion cells. In the present study, we used the patch-clamp technique to record γ -aminobutyric acid subtype A receptor-mediated miniature inhibitory postsynaptic currents in retinal ganglion cells from streptozotocin-induced diabetes model rats. We found that early diabetes (4 weeks of hyperglycemia) decreased the frequency of GABAergic miniature inhibitory postsynaptic currents in retinal ganglion cells without altering their amplitude, suggesting a reduction in the spontaneous release of γ -aminobutyric acid to retinal ganglion cells. Topical administration of glucagon-like peptide-1 eyedrops over a period of 2 weeks effectively counteracted the hyperglycemia-induced downregulation of GABAergic mIPSC frequency, subsequently enhancing the survival of retinal ganglion cells. Concurrently, the protective effects of glucagon-like peptide-1 on retinal ganglion cells in diabetic rats were eliminated by topical administration of exendin-9-39, a specific glucagon-like peptide-1 receptor antagonist, or SR95531, a specific antagonist of the γ -aminobutyric acid subtype A receptor. Furthermore, extracellular perfusion of glucagon-like peptide-1 was shown to elevate the frequencies of GABAergic miniature inhibitory postsynaptic currents in both ON- and OFF-type retinal ganglion cells. This elevation was shown to be mediated by activation of the phosphatidylinositol-phospholipase C/inositol 1,4,5-trisphosphate receptor/ Ca^{2+} /protein kinase C signaling pathway downstream of glucagon-like peptide-1 receptor activation. Moreover, multielectrode array recordings revealed that glucagon-like peptide-1 functionally augmented the photoresponses of ON-type retinal ganglion cells. Optomotor response tests demonstrated that diabetic rats exhibited reductions in visual acuity and contrast sensitivity that were significantly ameliorated by topical administration of glucagon-like peptide-1. These results suggest that glucagon-like peptide-1 facilitates the release of γ -aminobutyric acid onto retinal ganglion cells through the activation of glucagon-like peptide-1 receptor, leading to the de-excitation of retinal ganglion cell circuits and the inhibition of excitotoxic processes associated with diabetic retinopathy. Collectively, our findings indicate that the γ -aminobutyric acid system has potential as a therapeutic target for mitigating early-stage diabetic retinopathy. Furthermore, the topical administration of glucagon-like peptide-1 eyedrops represents a non-invasive and effective treatment approach for managing early-stage diabetic retinopathy.

Key Words: diabetic retinopathy; glucagon-like peptide-1; inhibitory synaptic transmission; miniature inhibitory postsynaptic currents; neurodegeneration; neuroprotection; patch-clamp recording; protein kinase C; signaling pathway; visual function

Introduction

Diabetic retinopathy (DR) is a prevalent complication of diabetes mellitus and a prominent cause of visual impairment and blindness globally (Leasher et al., 2016; Teo et al., 2021; GBD 2021 Diabetes Collaborators, 2023). In the brain, deficits in γ -aminobutyric acid (GABA) subtype A receptor (GABA_AR)-mediated neurotransmission are associated with a variety of pathophysiological and neurodegenerative diseases (Fritschy, 2008; Charych et al., 2009). GABA-modulating drugs have been used clinically as antiepileptic drugs, operating through the enhancement of inhibitory signals and the reduction of excitatory signals (Rogawski and Löscher, 2004). In the inner retina, inhibitory signaling

is processed through amacrine cells (ACs) and is primarily mediated by GABA. Increasing evidence indicates that diabetes induces the dysregulation of retinal neurotransmitters. For example, diabetes increases glutamate levels in the retina or vitreous (Ambati et al., 1997; Kowluru et al., 2001; Ali et al., 2019), suggesting that DR may be implicated in glutamate-induced excitotoxicity (Pulido et al., 2007). However, currently available evidence concerning changes in GABA after the induction of diabetes appears to be inconsistent. Although elevated GABA levels were found in the vitreous of patients with DR (Ambati et al., 1997; Barber and Baccouche, 2017), as well as in the retinas of diabetic model animals or cultured chicken retinas exposed to high-glucose conditions (Ishikawa et al., 1996; Miya-Coreixas et

State Key Laboratory of Medical Neurobiology and MOE Frontiers Center for Brain Science, Institutes of Brain Science, Fudan University, Shanghai, China

*Correspondence to: Yong-Mei Zhong, PhD, ymzhong@fudan.edu.cn.

<https://orcid.org/0000-0002-3382-2655> (Yong-Mei Zhong)

Funding: This study was supported by the National Natural Science Foundation of China, Nos. 32070989 (to YMZ), 31872766 (to YMZ), 81790640 (to XLY), and 82070993 (to SJW); and the grant from Sanming Project of Medicine in Shenzhen, No. SZSM202011015 (to XLY).

How to cite this article: Shao YQ, Wang YC, Wang L, Ruan HZ, Liu YF, Zhang TH, Weng SJ, Yang XL, Zhong YM (2026) Topical administration of GLP-1 eyedrops improves retinal ganglion cell function by facilitating presynaptic GABA release in early experimental diabetes. *Neural Regen Res* 21(2):800-810.



al., 2013; Carpi-Santos et al., 2017), other studies showed decreased GABA concentrations in retinas (Vilchis and Salceda, 1996; Honda et al., 1998). Furthermore, oscillatory potentials in electroretinograms, which indicate signal transduction between ACs and bipolar cells (Eggers and Carreon, 2020), are consistently altered in patients and animals with diabetes (Juen and Kieselbach, 1990; Layton et al., 2007; Luu et al., 2010; Zhang et al., 2011b; Pardue et al., 2014), suggesting changes in the inner retinal inhibitory system. *In vitro* studies of neuronal mechanisms have further focused on inhibitory inputs from ACs to rod bipolar cells (RBCs), demonstrating that, at the early stage of diabetes, light-evoked GABA release from GABAergic ACs to RBCs is reduced, whereas spontaneous GABA release to RBCs is increased (Moore-Dotson et al., 2016). Retinal ganglion cell (RGC)-mediated retinal output signals are regulated by GABA released from ACs to bipolar cells and RGCs (Masland, 2012). However, whether diabetes causes alterations in inhibitory input to RGCs remains unclear.

Owing to the intricate nature of its pathogenesis, there is a paucity of effective therapeutic strategies for DR. The development of drugs that can halt neurodegeneration is greatly anticipated. Glucagon-like peptide 1 (GLP-1), known for its neuroprotective role in various experimental models of neurodegenerative diseases (Salcedo et al., 2012; Koshal et al., 2018), experiences reductions in transcript and/or protein levels in the retinas of patients and rodents with diabetes (Hernández et al., 2016; Wang et al., 2023). Additionally, other studies including our own have shown that GLP-1 and GLP-1 receptor (GLP-1R) agonists protect retinal neurons, reduce L-type calcium currents in RGCs and vascular leakage, and prevent abnormal changes in electroretinogram oscillatory potentials and b-waves in diabetic animal models (Fan et al., 2014b; Hernández et al., 2016; Cai et al., 2017; Sampedro et al., 2019). Exendin-4, a widely used GLP-1R agonist, has also been demonstrated to enhance the frequency of GABA_AR-mediated miniature postsynaptic currents in hypocretin neurons in the lateral hypothalamus and gonadotropin-releasing hormone neurons (Acuna-Goycolea and van den Pol, 2004; Farkas et al., 2016). However, whether the GABA system is affected by GLP-1 in retinal neurons remains unknown.

Because GLP-1 exerts a hypoglycemic effect by stimulating glucose-dependent insulin secretion when administered systemically (Göke et al., 1993), it has been challenging to distinguish whether its neuroprotective effect is caused by lowering blood glucose levels or by directly activating GLP-1R in the retina. This problem could be addressed by topically administering GLP-1 via eyedrops, a convenient, noninvasive route of administration that does not appear to influence blood glucose levels. Here, we investigated the effects of diabetes on GABAergic synaptic transmission in the inner retina and examined the prevention of hyperglycemia-induced RGC loss by GLP-1 eyedrops via modulation of GABAergic synaptic transmission to RGCs.

Methods

Animals and diabetes induction

Male Sprague-Dawley rats (age: 4 weeks; weight: 80 g; specific pathogen free) were obtained from SLAC Laboratory Animal Company (Shanghai, China; license No. SCXK (Hu) 2022-0004). A total of 201 rats were used in this study. All procedures complied with the Association for Research in Vision and Ophthalmology (ARVO) Statement (ARVO, 2021) and were approved by the Bioethical Committee of Fudan University on March 6, 2020 (approval No. 20200306-145).

Because male rats exhibit heightened sensitivity to streptozocin compared with female rats, male rats were exclusively employed to minimize the overall number of animals used in the study. The diabetic rat model was established following the methodology outlined in our previous studies (Wang et al., 2013, 2023). After a 1-week acclimation, rats weighing approximately 100 g were randomly divided into two groups: the diabetic group was induced by intraperitoneal injection of streptozocin (70 mg/kg; Sigma-Aldrich, St. Louis, MO, USA) after fasting for 12 hours; the control group received injection of the vehicle (sodium citrate buffer). Blood glucose levels and body weights were monitored at various time points during the experiments (**Additional Figure 1**). Animals with blood glucose levels exceeding 16.7 mM were categorized as diabetic.

Topical ocular treatment

The detailed procedure for topical administration of drugs was described previously (Wang et al., 2023). Following 2 weeks of hyperglycemia, rats received

twice-daily ocular administration of eyedrops containing the following drugs or the vehicle (phosphate-buffered saline, PBS), applied onto the ocular surface of both eyes through the canthus, for 14 days: GLP-1 (2 mg/kg/d; MedChemExpress, Monmouth Junction, NJ, USA); exendin-9-39 (Ex-9-39, GLP-1R antagonist, 60 µg/kg/day; MedChemExpress) + GLP-1; or SR95531 (GABA_AR antagonist, 80 µg/kg/d, Sigma-Aldrich) + GLP-1. On day 15, the same eyedrops were administered 2 hours before the rats were prepared for optokinetic response testing. The rats were then sacrificed by intraperitoneal injection of 25% urethane (10 mL/kg, Sinopharm Chemical Reagent Co., Ltd, Shanghai, China) for morphologic examination or 2% pentobarbital sodium (2 mL/kg, Sigma-Aldrich) for electrophysiologic examination. Retinas were separated for immunofluorescence staining, patch-clamp recording, and multielectrode array (MEA) recording.

Enzyme-linked immunosorbent assays

Retinas, vitreous humor, ciliary bodies, and sclerae were harvested 1 or 2 hours after GLP-1 eyedrop administration for enzyme-linked immunosorbent assays (ELISAs) to measure GLP-1 penetration in ocular tissues. The isolated tissues were promptly frozen in liquid nitrogen and sonicated in lysis buffer (1:10 dilution; Beyotime, Shanghai, China) supplemented with a 1:200 dilution of protease inhibitor cocktail (P8340; Sigma-Aldrich). GLP-1 concentrations were quantified using the GLP-1 Multispecies ELISA Kit (BMS2194; Invitrogen, Carlsbad, CA, USA) following the manufacturer's instructions.

Labeling and counting of retinal ganglion cells

As described previously (Wang et al., 2023), rabbit anti-brain-specific homeobox/POU domain protein 3A (Brn3a) antibody (1:1000; Abcam, Cambridge, UK; Cat# ab245230, RRID: AB_2916038) was used to label RGCs in whole-mount rat retinas. Each retina was equally divided into four quadrants: nasal, temporal, dorsal, and ventral. Eight 256- × 256-µm areas (centered at 1 and 3 mm from the optic nerve head in each quadrant) of each retina were photographed, and cell counting was performed using ImageJ (version 1.54f). RGC density (cells/mm²) was evaluated in four peripheral areas and four central areas. A series of micrographs of the entire retina were automatically captured and reconstructed using a Nikon fluorescence microscope with a 20× objective lens (Eclipse Ni-U, Tokyo, Japan). The entire retinal area was delineated and measured using ImageJ software.

Retinal slice preparation and whole-cell patch-clamp recording

Rat retinal slices were meticulously prepared as previously outlined in detail (Ruan et al., 2021). The slices were continuously perfused with oxygenated artificial cerebrospinal fluid containing (in mM): 125 NaCl, 26 NaHCO₃, 1.25 NaH₂PO₄, 3 KCl, 1 MgCl₂, 2 CaCl₂, and 15 glucose, adjusted to pH 7.4 with NaOH.

Recording pipettes with 4–6 MΩ resistances were filled with an internal solution containing the following (in mM): 150 CsCl, 0.1 CaCl₂, 1 MgCl₂, 10 N-2-hydroxyethylpiperazine-N'-2-ethanesulfonic acid, 1 ethylene glycol-bis(2-aminoethyl ether)-N,N,N',N'-tetraacetic acid, 0.4 GTP-Na, 4 ATP-Mg, and 5 Lucifer yellow, adjusted to pH 7.3 with 1 M CsOH. Whole-cell recordings were conducted on RGCs with the voltage clamped at -60 mV. To isolate GABAergic miniature inhibitory postsynaptic currents (mIPSCs), QX-314 (4 mM) was included in the internal solution to block rapid Na⁺ currents, and the following drugs were added to the perfusate: tetrodotoxin (TTX, 0.5 µM; Tocris Bioscience, Ellisville, MO, USA), to eliminate spontaneous action potentials; and strychnine (10 µM; Sigma-Aldrich), 6,7-dinitroquinoxaline-2,3-dione (DNQX, 10 µM; Sigma-Aldrich), and D-2-amino-5-phosphonopentanoic acid (D-APV, 50 µM; Tocris Bioscience), to block glycine receptors, α-amino-3-hydroxy-5-methyl-4-isoxazolepropionic acid/kainic acid receptors, and N-methyl-D-aspartic acid receptors, respectively. The sampling frequency was set at 10 kHz and filtered at 3 kHz using a MultiClamp 700B amplifier (Molecular Devices, Palo Alto, CA, USA).

To distinguish RGCs from displaced ACs in the ganglion cell layer (GCL), we employed soma diameters as well as physiological criteria (Chen and Yang, 2007; Zhang et al., 2011a; Liu et al., 2015). Further identification of RGC subtypes was accomplished by analyzing light response characteristics, which were morphologically reconfirmed through cell injection with Lucifer yellow dye (Pang et al., 2003; Cui et al., 2019; Ruan et al., 2021).

Chemicals

TTX, strychnine, U-73122 (Sigma-Aldrich), bisindolylmaleimide IV

(Bis-IV; Sigma-Aldrich), 1,2-bis(2-aminophenoxy)ethane-N,N,N',N'-tetraacetic acid tetrakis (acetoxymethyl ester) (BAPTA-AM; Sigma-Aldrich), 2-aminoethoxydiphenyl borate (2-APB; Tocris Bioscience) and phorbol 12-myristate 13-acetate (PMA; Sigma-Aldrich) were initially dissolved in dimethyl sulfoxide to create stock solutions. The final concentration of dimethyl sulfoxide did not exceed 0.1%. Protein kinase C (19–36) [PKC (19–36), Sigma-Aldrich] was dissolved in intracellular solution. All other drug solutions were prepared in ddH₂O and drugs were diluted to final concentrations using extracellular solution.

Multielectrode array recording

The specific procedures for MEA referred to our previous work (Wang et al., 2023), with slight adjustments. Each separated retina was divided equally into four quadrants, with each quadrant cut into equal central and peripheral portions, placed photoreceptor-side down on a piece of Anodisc filter membrane. The retina was then positioned in the recording chamber of an MEA chip (60MEA200/30IR-ITO-gr; Multi Channel Systems GmbH, Reutlingen, Germany) with the GCL facing the array. Data were acquired using the USB MEA60-Inv-BC-System with MC Rack software (Multi Channel Systems). Raw electrical signals were digitized at 10 kHz, then amplified and filtered at 200 Hz. Full-field stimulation of the retina was performed using a custom-made fiber-optic light emitting diode illuminator (Model 66991; DiCon Fiberoptics Inc., Richmond, CA, USA) to generate 1-second, 500-nm light flashes. The light intensity ranged from 1.51×10^6 to 3.04×10^{12} photons/cm²/s.

Spike sorting was executed following a previously established protocol (Weng et al., 2009). RGCs were classified on the basis of their spiking pattern in response to light stimuli, as characterized by the Response Dominant Index (Tian and Copenhagen, 2003). Two parameters were statistically analyzed: spontaneous firing rate (the average firing frequency in the 1 second preceding the light onset) and light-evoked maximum (peak) firing rate calculated at 50-ms intervals during a 1-second period following light onset (ON-RGCs) or offset (OFF-RGCs).

Visual acuity and contrast sensitivity measurement

Visual function of each animal was tested using a homemade virtual optokinetic system, as previously detailed (Yang et al., 2023). Briefly, the rat was positioned on a platform enclosed by four liquid-crystal monitors that displayed a visual stimulus in the form of rotating black and white gratings at a speed of 12 degrees/s. The drifting gratings rotated both clockwise and counterclockwise for 10 seconds, and were repeated three times. To evaluate spatial frequency thresholds, the grating contrast was held at 100%, starting with a spatial frequency of 0.031 cycles per degree (cpd) and increasing in steps of 0.05 cpd until the rat did not exhibit head-tracking movements. A valid head tracking trial was characterized by the presence of slow angular head movements in response to the rotating grating (Douglas et al., 2005; Yang et al., 2023). The maximum spatial frequency of drifting grating capable of driving head tracking was identified as visual acuity.

The contrast sensitivity was determined by decreasing the grating contrast from 100%, in steps of 5%, until the rat did not exhibit head-tracking movements. Contrast sensitivity was measured at different spatial frequencies (0.031, 0.045, 0.064, 0.092, 0.130 and 0.192 cpd). The lowest contrast of drifting grating at which the rat had head-tracking movement was determined as the contrast threshold. The contrast sensitivity at each spatial frequency was determined by taking the reciprocal of the contrast threshold.

Statistical analysis

Data were analyzed using Excel 2016 (Microsoft, Redmond, WA, USA), MiniAnalysis 6.0.3 (Bioz, Los Altos, CA, USA), and GraphPad prism 8.0.0 for Windows (GraphPad Software, San Diego, CA, USA, www.graphpad.com). Based on the type and distribution of the data, we identified significant differences using paired *t*-test, unpaired *t*-test, Mann–Whitney *U* test, Kruskal–Wallis *H* test followed by Dunn's multiple comparisons test, one-way analysis of variance (ANOVA) with Tukey's multiple comparisons test, one-way repeated measures ANOVA with Tukey's multiple comparisons test, and two-way ANOVA with Tukey's multiple comparisons test or Sidak's multiple comparisons test. Data are presented as mean ± standard error of mean (SEM), except for the spontaneous action potential firing rates of RGCs in the MEA experimental results, which are presented as medians ± interquartile range (IQR). A *P* value < 0.05 was considered to indicate statistical significance.

Results

Glucagon-like peptide-1 increases GABAergic miniature inhibitory postsynaptic currents frequency in retinal ganglion cells

Because GABAergic ACs send projections to RGCs, we first tested the effect of GLP-1 on GABAergic synaptic transmission onto RGCs in normal rats. To isolate and identify GABAergic mIPSCs, we recorded from RGCs with extracellular perfusion of 50 μM D-APV, 10 μM DNQX, 10 μM strychnine, and 0.5 μM TTX to block α-amino-3-hydroxy-5-methyl-4-isoxazolepropionic acid/kainic acid receptor, N-methyl-D-aspartic acid receptor, glycine receptor, and spontaneous action potentials; 4 mM QX-314 was included in the internal perfusion solution to eliminate sodium currents (**Additional Figure 2**). The mIPSCs were almost eliminated ($4.48\% \pm 1.86\%$ of control) by perfusion of 10 μM SR95531, a specific GABA_AR antagonist, suggesting that the currents were mediated by GABA_AR. The roles of GLP-1 in modulating mIPSCs of RGCs were investigated following the protocol illustrated in **Figure 1A**. **Figure 1B** and **C** show the effects of extracellular perfusion of GLP-1 (10 nM) on mIPSCs of an ON-RGC. GLP-1 reversibly increased the mIPSC frequency in ON-RGCs, with the average frequency being increased from 1.24 ± 0.18 Hz to 1.67 ± 0.19 Hz ($P = 0.0121$; **Figure 1D**). Similarly, 10 nM GLP-1 increased the mIPSC frequency of OFF-RGCs from 0.32 ± 0.05 Hz to 0.57 ± 0.05 Hz ($P = 0.0072$; **Figure 1F–H**). However, GLP-1 failed to alter the mIPSC amplitude in either type of RGC (**Figure 1E** and **I**). Because the effects of GLP-1 on mIPSCs were not significantly different between the two types of RGCs, data from both types were pooled in the subsequent study. Statistical analysis of a total of 26 recorded RGCs showed that the average frequency of mIPSCs was increased to $183\% \pm 23\%$ of the control ($P = 0.0004$; **Figure 1J**).

We also examined the effects of different concentrations of GLP-1 on mIPSCs of RGCs. As shown in **Figure 1K**, following application of GLP-1 at 5, 10, and 100 nM, the mIPSC frequencies were increased to $(157 \pm 16)\%$ ($P = 0.0056$), $(183 \pm 23)\%$ ($P = 0.0016$), and $(152 \pm 19)\%$ of the control ($P = 0.0181$), respectively. Lower (0.05 or 0.5 nM) or higher (1000 nM) concentrations of GLP-1 did not change the mIPSC frequency, exhibiting a bell-shaped concentration-response relationship. This finding is consistent with the concentration-response relationship of GLP-1 previously reported in hippocampal CA3 pyramidal cells (Korol et al., 2015).

Glucagon-like peptide-1 improves diabetes-related reductions in GABAergic miniature inhibitory postsynaptic currents frequency

Next, we investigated whether early diabetes (4 weeks of hyperglycemia) would cause changes in mIPSCs of rat RGCs. Compared with control RGCs, hyperglycemia induced significant decreases in mIPSC frequency in both ON-RGCs ($52.56\% \pm 10.57\%$ of control) and OFF-RGCs ($48.18\% \pm 7.05\%$ of control, data not shown). When the ON-RGC and OFF-RGC data were pooled, the results showed that the mIPSC frequency in the diabetic group (DM; 0.44 ± 0.04 Hz) decreased to $46.6\% \pm 4.57\%$ of the control group (0.95 ± 0.08 Hz, $P < 0.0001$; **Figure 2A** and **B**). Perfusion of GLP-1 significantly increased the mIPSC frequency of diabetic RGCs to 0.71 ± 0.18 Hz ($P = 0.0359$ vs. DM; **Figure 2B**), but neither hyperglycemia nor GLP-1 had an effect on the amplitudes of mIPSCs (**Figure 2C**). Diabetic RGCs also responded to GLP-1 in a concentration-dependent manner and were more sensitive to GLP-1 than control ones. For the diabetic RGCs, GLP-1 concentration as low as 0.05 nM still significantly increased mIPSC frequency to $164\% \pm 17\%$ of control ($P = 0.0326$), with a range of effective GLP-1 concentration of 0.05–10 nM (**Figure 2D**). By contrast, the effective concentration of GLP-1 in normal RGCs was 5–100 nM (**Figure 1K**).

To investigate the influence of topical administration of GLP-1 eyedrops on diabetic rats, we first tested the ability of GLP-1 to reach the retina. GLP-1 levels in the retina were significantly increased at 1 hour (102.7 ± 1.27 ng/g, $P = 0.0017$ vs. PBS) and 2 hours (85.62 ± 16.96 ng/g, $P = 0.005$ vs. PBS) post GLP-1 administration (**Additional Figure 3A**). Next, GLP-1 (2 mg/kg/d) was administered by eyedrops to rats at 2 weeks post streptozocin induction, twice a day for 2 weeks (**Figure 2E**). While this dosing of GLP-1 eyedrops did not affect blood glucose levels or body weight in diabetic rats (**Additional Figure 3B** and **C**), it did enhance the mIPSC frequency of diabetic RGCs (**Figure 2F**). Statistical analysis showed that the mIPSC frequency was significantly higher in the DM + GLP-1 group (0.87 ± 0.14 Hz) than in the DM + PBS (vehicle) group (0.39 ± 0.11 Hz, $P = 0.011$; **Figure 2G**), but the mIPSC amplitude remained unchanged (**Figure 2H**).

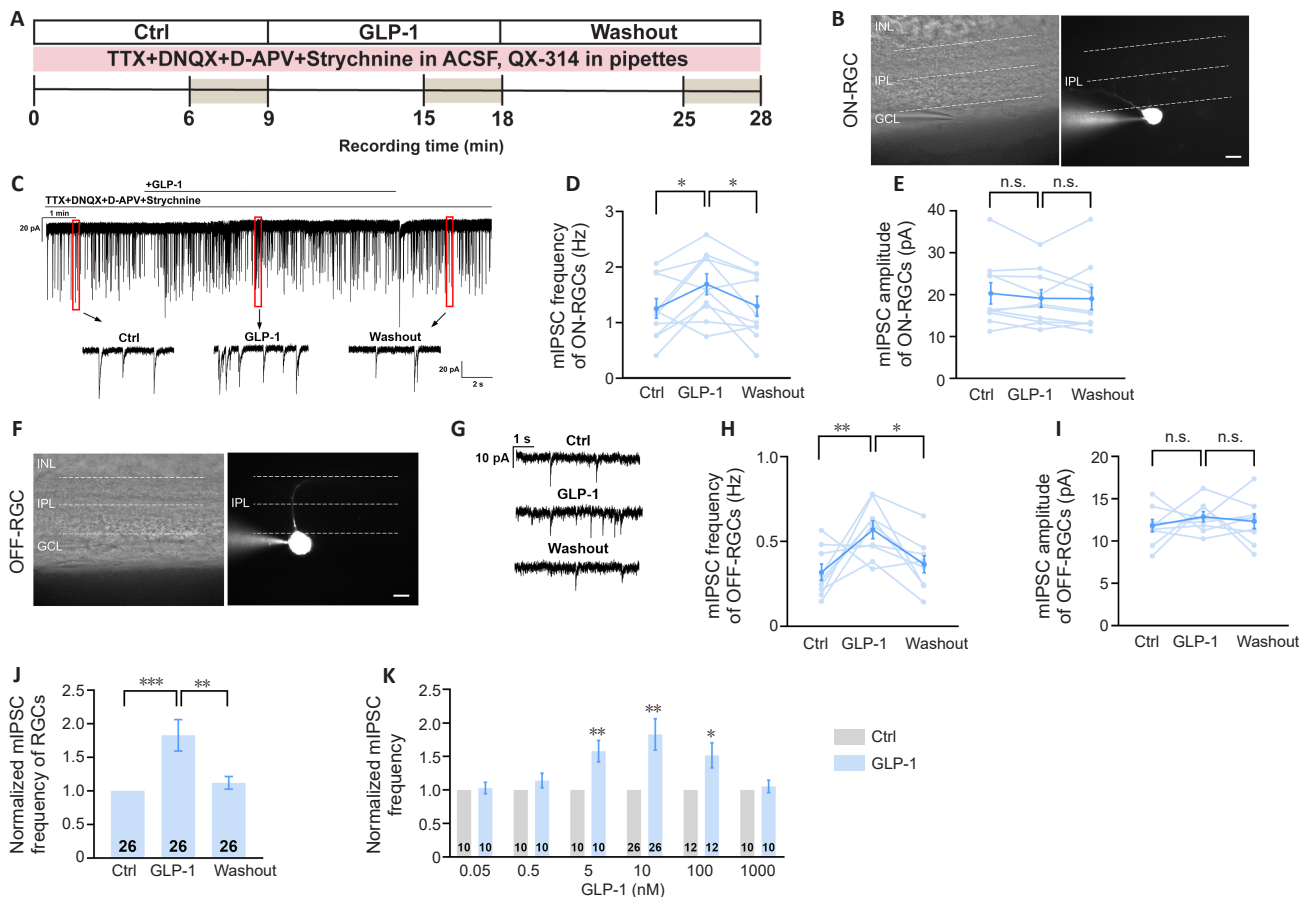


Figure 1 | GLP-1 enhances mIPSCs of normal RGCs in a concentration-dependent manner.

(A) Schematic illustration of the experimental protocol for continuously recording mIPSCs from an RGC for 28 minutes. Data were statistically analyzed at the following time periods: 6–9 minutes of Ctrl, 15–18 minutes of GLP-1 application, and 25–28 minutes of washout. (B) Micrographs of the same retinal section taken with an infrared interferometric phase microscope (left) and a fluorescence microscope (right), showing a representative Lucifer yellow dye-filled ON-RGC with dendrite arborizations in the proximal part of the IPL. Scale bar: 10 μ m. (C) Representative current traces showing the effect of 10 nM GLP-1 on GABAergic mIPSCs of an ON-RGC (top trace) and the mIPSC currents on an expanded time scale (bottom traces). (D, E) Scatterplots of mIPSC frequency and amplitude from individual recordings, demonstrating a GLP-1-mediated reversible increase in mIPSC frequency (D), but not amplitude (E) in ON-RGCs ($n = 10$). (F) Representative micrographs showing a typical Lucifer yellow-filled OFF-RGC with dendrite arborizations in the distal part of the IPL. Scale bar: 10 μ m. (G) Current traces showing the effect of GLP-1 on mIPSCs of an OFF-RGC. (H, I) GLP-1 reversibly increased mIPSC frequency (H), but not amplitude (I) in OFF-RGCs ($n = 9$). (J) Normalized mIPSC frequency recorded in 26 RGCs. (K) Increases in mIPSC frequencies under GLP-1 concentrations of 5, 10, and 100 nM, but not 0.05, 0.5, or 1000 nM. All data normalized to the control values obtained before GLP-1 application. Cell numbers are marked inside the bars in panels J and K. Data are presented as mean \pm SEM; * $P < 0.05$, ** $P < 0.01$, *** $P < 0.001$, determined by one-way repeated measures analysis of variance with Tukey's multiple comparisons test (D, E, H–J) and paired t -test (K). ACSF: Artificial cerebrospinal fluid; Ctrl: control; D-APV: D-2-amino-5-phosphonopentanoic acid; DNQX: 6,7-dinitroquinoxaline-2,3-dione; GABA: γ -aminobutyric acid; GCL: ganglion cell layer; GLP-1: glucagon-like peptide-1; INL: inner nuclear layer; IPL: inner plexiform layer; mIPSC: miniature inhibitory postsynaptic current; RGC: retinal ganglion cell; TTX: tetrodotoxin.

We also explored the delivery route of GLP-1 using ELISAs. GLP-1 levels in the sclera and ciliary body were markedly increased at 1 and 2 hours post-GLP-1 eyedrop administration, but the GLP-1 level in the vitreous humor was minimal (Additional Figure 3A). These results suggested that GLP-1 eyedrops most likely reach the retina through the trans-scleral route, not through the cornea.

Topical administration of glucagon-like peptide-1 protects diabetic retinal ganglion cells

To determine whether potentiation of mIPSCs by GLP-1 could promote RGC survival, we used the RGC-specific marker Brn3a antibody to label surviving RGCs in whole-mount retinas. Beginning 2 weeks after streptozocin induction, rats were treated with eyedrops containing PBS, GLP-1, Ex-9-39 + GLP-1, or SR95531 + GLP-1, administered twice a day for 2 weeks (refer to Figure 2E), and then the number of Brn3a-labeled RGCs was counted. Representative images of the central and peripheral retinal areas in each group are shown in Figure 3A1–A6 and B1–B6. RGC density was evaluated in four peripheral areas (Figure 3C) and four central areas (Figure 3E), as indicated by pink squares in the respective figure panels. Statistical analyses showed significant differences in RGC density in the peripheral (Figure 3D) and central areas (Figure 3F) among the six groups (peripheral: $P < 0.0001$; central: $P = 0.0013$). The RGC density in the peripheral area was significantly lower in diabetic retinas (1311 ± 62.66 cells/ mm^2) than in control retinas (1782 ± 36.07 cells/ mm^2) ($P < 0.0001$; Figure 3D).

Furthermore, the RGC density in the peripheral area was significantly higher in DM + GLP-1 retinas (1696 ± 49.52 cells/ mm^2) than in DM + PBS retinas (1306 ± 70.4 cells/ mm^2 ; $P < 0.0001$). These results indicated that GLP-1 eyedrops significantly promoted RGC survival in diabetic rat eyes.

To investigate the potential involvement of GLP-1R in these effects, diabetic rats were treated with eyedrops containing Ex-9-39 (60 μ g/kg/d) and GLP-1 (2 mg/kg/d). The RGC density in the peripheral retinal area in GLP-1 + Ex-9-39-treated diabetic eyes was 1095 ± 54.55 cells/ mm^2 , which was significantly lower than that in GLP-1-treated diabetic eyes ($P < 0.0001$), and was similar to that in PBS-treated diabetic eyes ($P = 0.0986$; Figure 3D). To further confirm the protective effect of GLP-1 through the GABA system, we examined the effects of GLP-1 eyedrops containing SR95531 (80 μ g/kg/d) eyedrops, a specific GABA_AR antagonist. SR95531 eliminated the protective effect of GLP-1 on RGCs in diabetic rats, decreasing the cell density in the peripheral area to 1331 ± 41.41 cells/ mm^2 ($P < 0.0001$ vs. DM + GLP-1; Figure 3D).

Unlike the peripheral retinal area, 4 weeks of hyperglycemia did not significantly alter the mean RGC density in the central retinal area ($P = 0.1366$ vs. control; Figure 3F). Notably, in the central region, only the DM + Ex-9-39 + GLP-1 group had a significantly lower RGC density (2133 ± 118 cells/ mm^2) than the control group (2592 ± 53.53 cells/ mm^2 , $P = 0.0026$; Figure 3F). We speculate that Ex-9-39 may abolish the protective effect of endogenous GLP-1, thus exacerbating RGC damage in early diabetes.

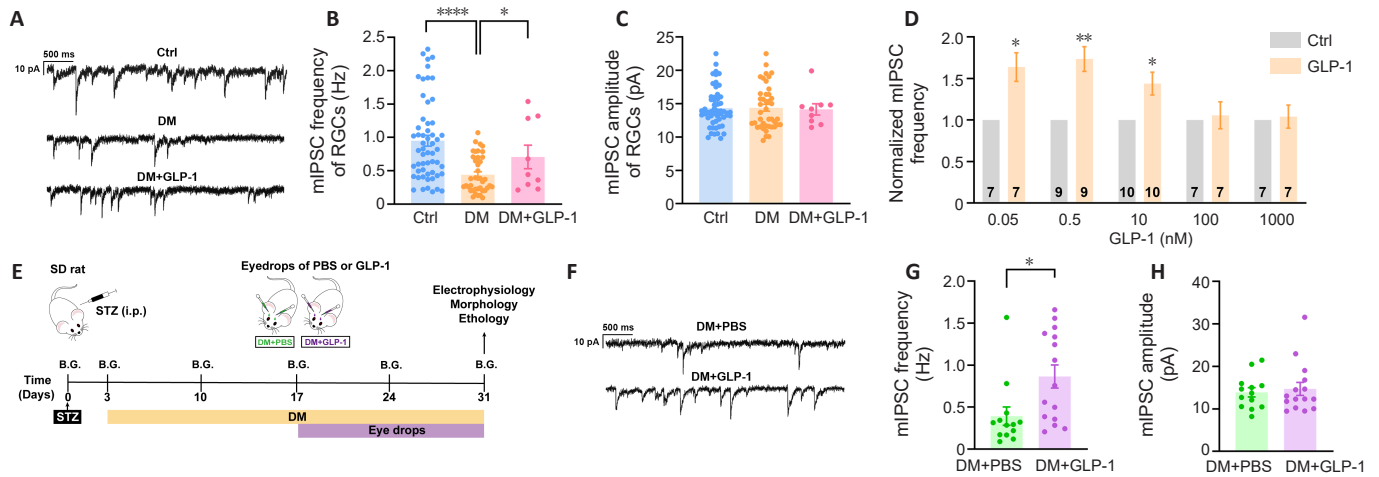


Figure 2 | GLP-1 reverses the hyperglycemia-induced reduction in the mIPSC frequency of RGCs.

(A) Representative mIPSC traces recorded from RGCs in Ctrl and DM group retinas before and after perfusion of 10 nM GLP-1 (DM + GLP-1). (B, C) Bar charts summarizing the changes in mIPSC frequency (B) and amplitude (C) of RGCs from Ctrl ($n = 56$), DM ($n = 40$), and DM + GLP-1 ($n = 9$) group retinas. (D) mIPSC frequencies increased upon GLP-1 application at 0.05, 0.5 and 10 nM, but not 100 and 1000 nM. Cell numbers are marked inside the bars. (E) Schematic illustration of the experimental procedure and data collection schedule. Two weeks after streptozocin induction, rats received GLP-1 eyedrops or PBS eyedrops twice a day for 2 weeks, followed by preparations for further experiments. (F) Representative mIPSC traces recorded from an RGC of a diabetic rat treated with PBS eyedrops (DM + PBS) and an RGC of a diabetic rat treated with GLP-1 eyedrops (DM + GLP-1). (G, H) Bar charts summarizing the changes in mIPSC frequency (G) and amplitude (H) of RGCs from DM + PBS ($n = 13$) and DM + GLP-1 ($n = 15$) group retinas. Data are presented as mean \pm SEM; $*P < 0.05$, $**P < 0.01$, $***P < 0.0001$, determined by unpaired t -test (B and C), paired t -test (D), and Mann–Whitney U test (G and H). B.G.: The time point at which the blood glucose level was measured; Ctrl: control; DM: diabetes mellitus; GLP-1: glucagon-like peptide-1; i.p.: intraperitoneal injection; mIPSC: miniature inhibitory postsynaptic current; PBS: phosphate-buffered saline; RGC: retinal ganglion cell; STZ: streptozocin.

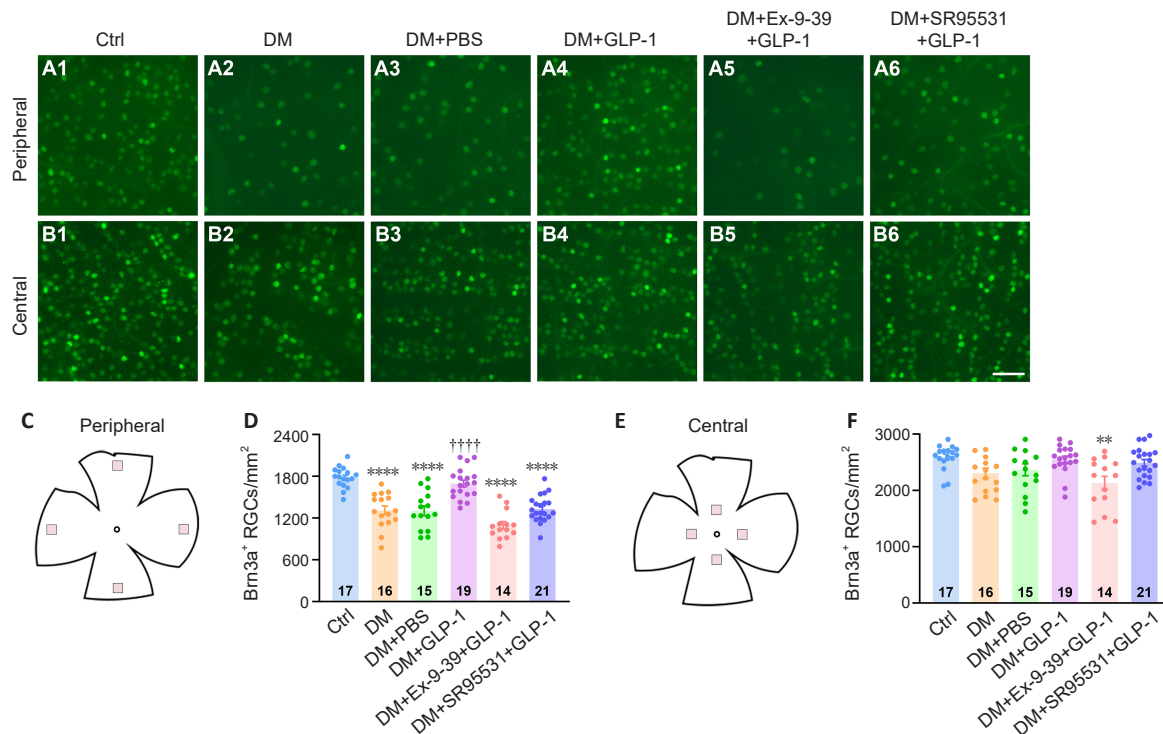


Figure 3 | Topical administration of GLP-1 promotes the survival of diabetic RGCs.

(A, B) Representative fluorescence micrographs from the peripheral and central regions of flat-mount retinas showing Brn3a-positive surviving RGCs in the following groups: control (Ctrl; A1, B1); diabetic (DM; A2, B2); diabetic rats treated with PBS (DM + PBS; A3, B3), GLP-1 (DM + GLP-1; A4, B4), Ex-9-39 + GLP-1 (DM + Ex-9-39 + GLP-1; A5, B5), and SR95531 + GLP-1 (DM + SR95531 + GLP-1; A6, B6). Scale bar: 50 μ m. (C, E) Schematic diagrams of flat-mount retinas showing the eight areas targeted for RGC counting: four peripheral and four central, as indicated by pink squares. (D, F) Quantitative analysis of RGC density in the peripheral (D) and central (F) regions of retinas from the six treatment groups. Retina numbers are noted in the bars. Data are presented as mean \pm SEM; $**P < 0.01$ and $****P < 0.0001$ vs. Ctrl group, and $++++P < 0.0001$ vs. DM + PBS group, determined by one-way analysis of variance with Tukey’s multiple comparisons test. Ex-9-39: Exendin-9-39, GLP-1 receptor antagonist; GLP-1: glucagon-like peptide-1; PBS: phosphate-buffered saline; RGC: retinal ganglion cell; SR95531: γ -aminobutyric acid sub-type A receptor antagonist.

We also measured total retinal area, which was similar in the DM (57.5 ± 0.86 mm²) and control (59.02 ± 0.9 mm²) groups ($P = 0.2317$; **Additional Figure 4**). Taken together, our data suggested that 4 weeks of hyperglycemia induced a significant decrease in RGC density in the peripheral retinal area, whereas

administration of GLP-1-containing eyedrops promoted RGC survival, and this effect was mediated by GLP-1R and GABA_AR. Additionally, the effect of hyperglycemia on RGCs was stronger in the peripheral area than in the central area of the retina.

Glucagon-like peptide-1R mediates the glucagon-like peptide-1 effect on miniature inhibitory postsynaptic currents

Next, we sought to further explore the role of GLP-1R in the GLP-1 effect on GABAergic mIPSCs. Prior to the application of Ex-9-39, we confirmed that GLP-1 increased the mIPSC frequency in the RGC recorded (Figure 4A). After washout, the current frequency returned to the control level and the RGC was perfused with Ex-9-39 for 6 minutes. Ex-9-39 alone did not change the mIPSC frequency (96% ± 4% of control, $P = 0.93$), and co-application of GLP-1 for a further ~6 minutes no longer affected the mIPSC frequency (96% ± 6% of control, $P = 0.9406$; Figure 4B). However, neither of these chemicals affected the mIPSC amplitude (Figure 4C). These results suggested that GLP-1 potentiates presynaptic inhibitory neurotransmission to RGCs via GLP-1R activation.

Intracellular signaling pathway underlying the glucagon-like peptide-1-induced potentiation of miniature inhibitory postsynaptic currents

The phospholipase C (PLC)/protein kinase C (PKC) signaling pathway has been shown to be a downstream target of activated GLP-1R in pancreatic β cells (Shigeto et al., 2017). The possible contribution of this pathway to the GLP-1 effect on mIPSCs was investigated using the phosphoinositide (PI)-PLC inhibitor U73122. Perfusion of 10 μ M U73122 for 10 minutes did not affect frequencies or amplitudes of mIPSCs (Figure 5A–C). It also had no impact on mIPSC frequency (90% ± 6% of control, $P = 0.1231$; Figure 5B) or amplitude (94% ± 8% of control, $P = 0.3786$; Figure 5C) in co-application with GLP-1, suggesting involvement of the PI-PLC pathway.

Because Ca^{2+} signaling is thought to link PI-PLC and PKC (Monnet, 2005), we investigated the possible influence of intracellular Ca^{2+} concentration on GLP-1-mediated effects. Perfusion of 50 μ M BAPTA-AM, a membrane-permeable chelator of presynaptic Ca^{2+} , suppressed the mIPSC frequency to 35% ± 6% of control ($P < 0.0001$; Figure 5D and E), and provision of additional GLP-1 no longer increased the mIPSC frequency (33% ± 5% of control, $P = 0.9222$ vs. BAPTA-AM). By contrast, perfusion of BAPTA-AM either alone (99% ± 6% of control, $P = 0.9717$) or co-applied with GLP-1 (101% ± 6% of control, $P = 0.9938$) did not affect the mIPSC amplitude (Figure 5F). These results indicated that the GLP-1 effect is dependent on the presynaptic Ca^{2+} concentration.

Release of Ca^{2+} from intracellular calcium pools is mediated by ryanodine-and/or 1,4,5-trisphosphate (IP_3) receptors (IP_3 R). Because PLC catalyzes the decomposition of phosphoinositol 4,5-bisphosphate into IP_3 and diacylglycerol (Kiselyov et al., 2003), we tested the effect of 2-APB, a membrane-permeable IP_3 R antagonist on RGCs. Perfusion of 2-APB (50 μ M) decreased the mIPSC frequency to 40% ± 9% of control ($P < 0.0001$; Figure 5G and H), and the provision of additional GLP-1 no longer increased the frequency (38% ± 7% of control, $P = 0.9476$ vs. 2-APB), suggesting that the GLP-1 effect is dependent on IP_3 R-mediated release of Ca^{2+} from intracellular calcium pools. The mIPSC amplitude in these RGCs was not impacted by 2-APB (90% ± 6% of control, $P = 0.2419$) or 2-APB + GLP-1 (88% ± 7% of control, $P = 0.1401$) (Figure 5I).

PKC is activated by PLC-generated diacylglycerol together with IP_3 R-mediated Ca^{2+} release (Boni and Rando, 1985). We used the PKC inhibitor Bis-IV to test the possible involvement of PKC in GLP-1-mediated effects. Bis-IV (10 μ M) did not impact the frequency or amplitude of mIPSCs either alone or in co-application

with GLP-1 (102% ± 6% of control, $P = 0.8817$ and 97% ± 5% of control, $P = 0.8708$, respectively; Figure 5J–L). By contrast, perfusion of the PKC activator PMA (1 μ M) significantly increased the mIPSC frequency (138% ± 8% of control, $P = 0.0005$; Figure 5M and N), but had no effect on the amplitude (95% ± 5% of control, $P = 0.4454$; Figure 5O). Provision of GLP-1 during perfusion of PMA did not further increase mIPSC frequency (136% ± 9% of control, $P = 0.9812$ vs. PMA).

To exclude the effect of postsynaptic PKC, we added PKC (19-36), a membrane-impermeable PKC antagonist, into the internal perfusion solution to limit the action of PKC antagonist on postsynaptic RGCs. Using an internal perfusion solution containing 50 μ M PKC (19-36), GLP-1 still significantly increased mIPSC frequency (160% ± 16% of control, $P = 0.0036$; Figure 5P and Q), with no effect on mIPSC amplitude (100% ± 7% of control, $P = 0.9566$; Figure 5R).

Glucagon-like peptide-1 improves diabetes-induced functional impairment of retinal ganglion cells

The ability to respond to light is the most important physiological function of RGCs (Masland, 2001). Using MEA recordings, we examined light responses to determine whether 4 weeks of hyperglycemia leads to functional impairment of RGCs. Figure 6A shows representative raster plots of light-evoked spikes of ON-RGCs and OFF-RGCs in the peripheral and central retinal areas recorded by MEA at a light intensity of 1.49×10^9 photons/cm²/s. We measured the spontaneous firing rate in RGCs within 1 second before the delivery of a light stimulus in the control, DM, DM + PBS, and DM + GLP-1 groups; however, because the data showed non-normal distributions, we used box and whisker plots for quantitative comparisons. In the peripheral retina, the spontaneous firing rate of ON-RGCs was significantly higher in the DM group (median: 11.13 Hz, IQR: 6.59–19.97 Hz) compared with that in the control group (median: 6.38 Hz, IQR: 3.42–8.5 Hz, $P = 0.0059$; Figure 6B). Similarly, ON-RGCs in the central retina also exhibited a higher spontaneous firing rate in the DM group (median: 10.86 Hz, IQR: 7.71–20.7 Hz) compared with that in the control group (median: 6.25 Hz, IQR: 4–10.63 Hz, $P = 0.038$; Figure 6C). Treatment of diabetic rat eyes with GLP-1 eyedrops significantly reduced the spontaneous firing rate of ON-RGCs in both the peripheral (median: 3.57 Hz, IQR: 2.14–5.86 Hz, $P = 0.0001$) and central (median: 3.29 Hz, IQR: 1.51–4.71 Hz, $P = 0.0002$) retinas compared with that in PBS-treated diabetic eyes (median: 9 Hz and IQR: 4–22.13 Hz in peripheral retina; median: 7.57 Hz and IQR: 5.43–14.5 Hz in central retina; Figure 6B and C). By contrast, no significant differences in spontaneous firing rate were detected in OFF-RGCs in either the peripheral ($P = 0.2231$) or central ($P = 0.2005$) retinas among the four groups (Figure 6D and E).

The peak firing rate of light-evoked spikes of ON-RGCs rose with increasing light intensity in the control, DM, DM + PBS, and DM + GLP-1 groups (Figure 6F–I). Irradiance-response (I–R) curves revealed a significant downward shifting in the peak firing rate of diabetic ON-RGCs in both peripheral ($P < 0.0001$) and central ($P = 0.0378$) retinas compared with those in the corresponding control retinas (Figure 6F and H). By contrast, I–R curves of ON-RGCs in DM + GLP-1 rats shifted significantly upward (peripheral: $P < 0.0001$; central: $P = 0.0008$) compared with those of DM + PBS group ON-RGCs, suggesting that treatment with GLP-1 eyedrops increased response gain (Figure 6F and H). In OFF-RGCs of all groups, the peak firing rate in both the peripheral and central retinal regions remained unchanged (Figure 6G and I).

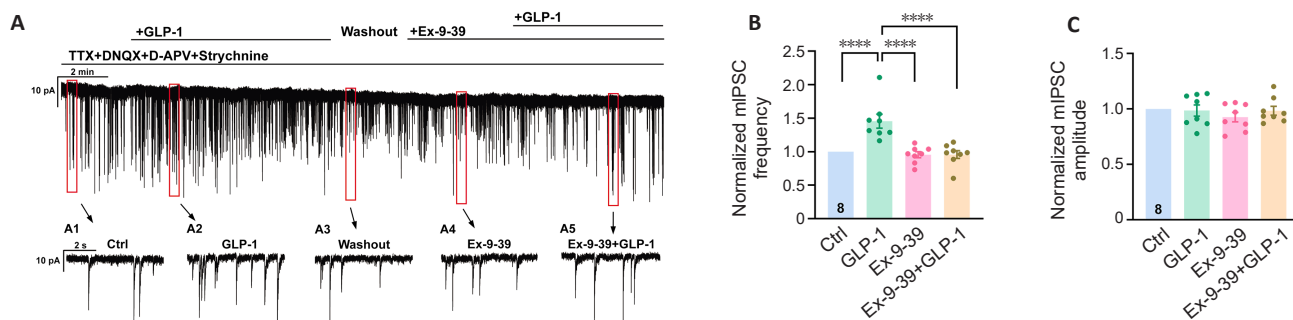


Figure 4 | GLP-1-induced increase in mIPSC frequency is blocked by Ex-9-39.

(A) Representative recordings of an RGC (top trace) after the application of TTX + DNQX + D-APV + strychnine, showing Ex-9-39-mediated blockage of GLP-1-induced changes in mIPSC frequency. The bottom traces (A1–A5) show the currents on an expanded time scale. A1, control condition; A2, GLP-1 application; A3, washout; A4, Ex-9-39 application; and A5, Ex-9-39 + GLP-1 application. (B, C) Bar charts showing statistical analyses of the mIPSC frequency (B) and amplitude (C) ($n = 8$) under the different conditions. Data (normalized by the Ctrl group) are presented as mean ± SEM; **** $P < 0.0001$, determined by one-way repeated measures analysis of variance with Tukey’s multiple comparisons test. Ctrl: Control; D-APV: D-2-amino-5-phosphonopentanoic acid; DNQX: 6,7-dinitroquinoxaline-2,3-dione; Ex-9-39: exendin-9-39, GLP-1 receptor antagonist; GLP-1: glucagon-like peptide-1; mIPSC: miniature inhibitory postsynaptic current; RGC: retinal ganglion cell; TTX: tetrodotoxin.

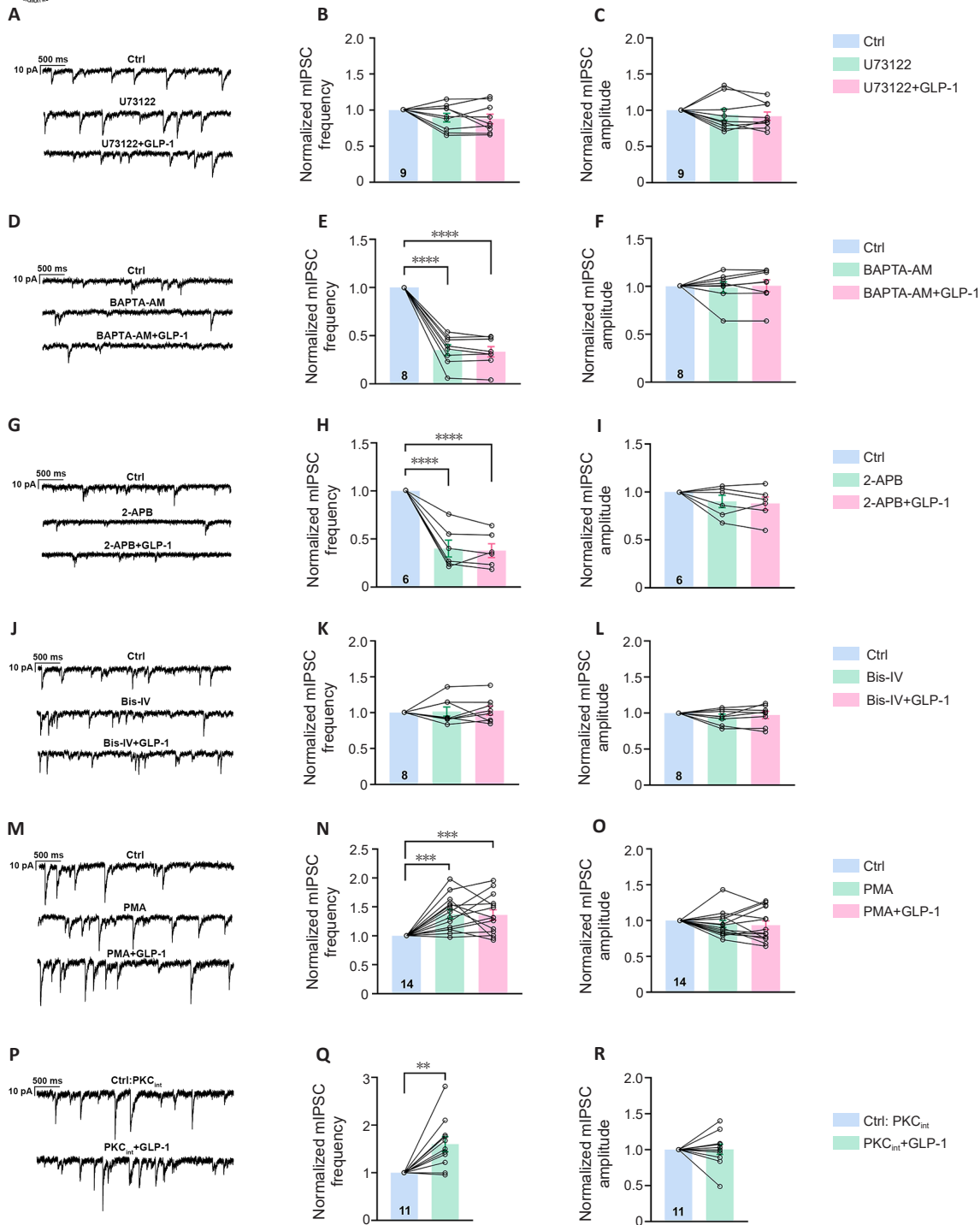


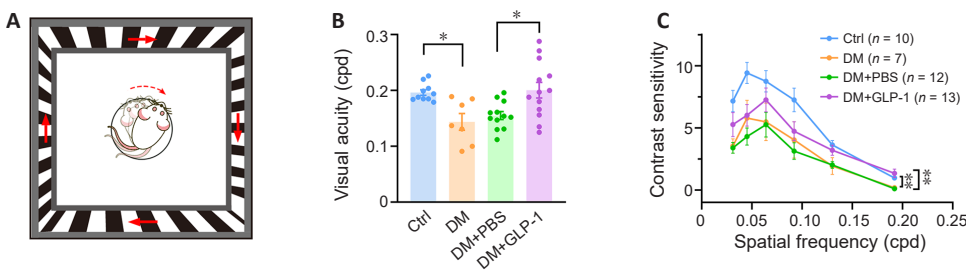
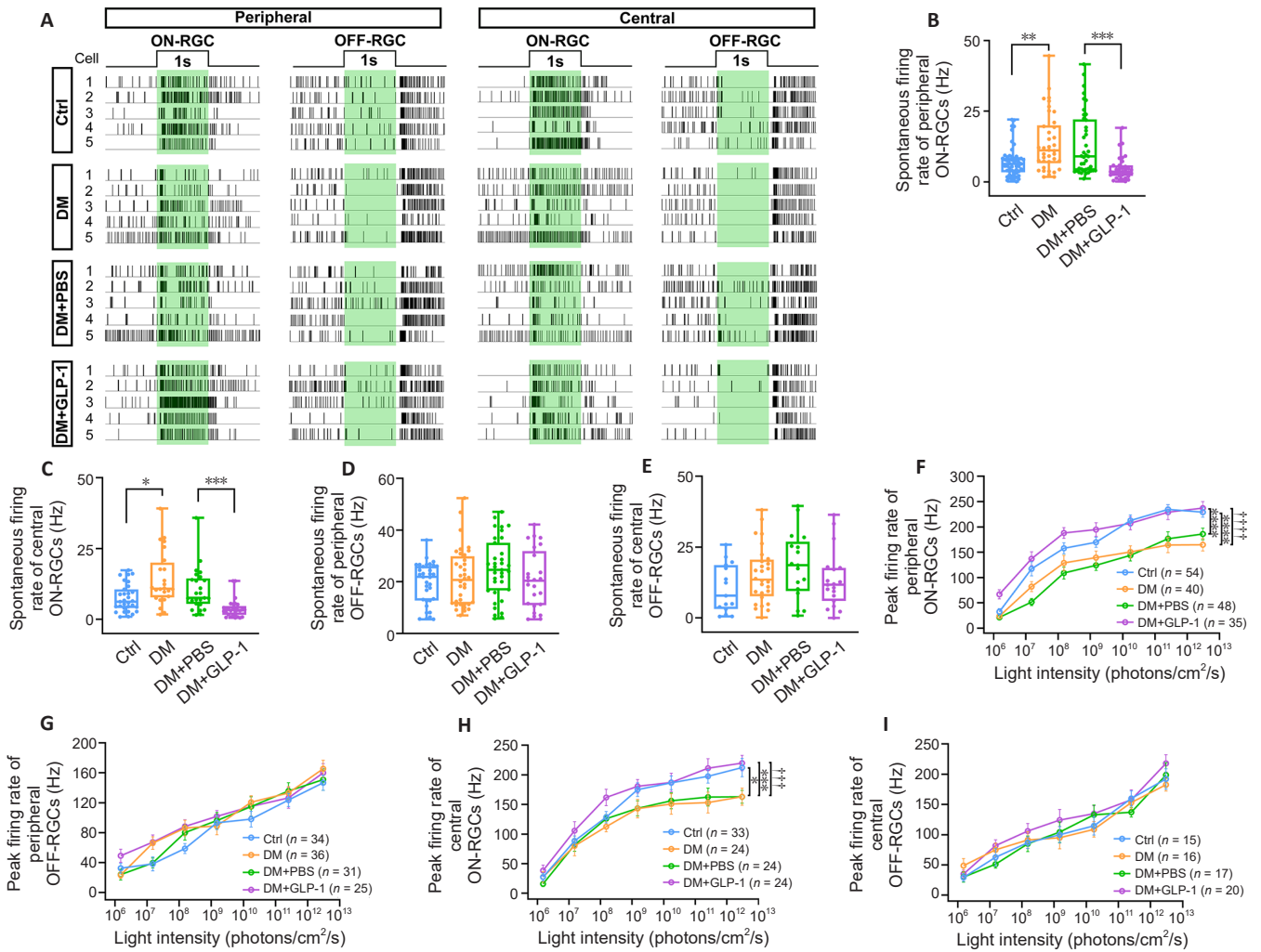
Figure 5 | Involvement of the PI-PLC/IP₃R/Ca²⁺/PKC signaling pathway in the GLP-1-induced potentiation of mIPSCs.

(A–C) Representative recordings of an RGC in the presence of 10 μM U73122, with or without 10 μM GLP-1 (A), and summary data of mIPSC frequency (B) and amplitude (C) ($n = 9$). (D, G) Representative traces of mIPSCs recorded from two RGCs, showing that chelating presynaptic Ca²⁺ with 50 μM BAPTA-AM (D) or blocking IP₃R with 50 μM 2-APB (G) reduced the mIPSC frequency and prevented the GLP-1-mediated increase in mIPSC frequency. (E, F, H, I, K, L) Bar charts summarizing the effects of BAPTA-AM ($n = 8$; E, F), 2-APB ($n = 6$; H, I), Bis-IV ($n = 8$; K, L), and GLP-1 on mIPSC frequency and amplitude. (J) Representative recordings of an RGC showing the failure of GLP-1 to increase mIPSC frequency in the presence of 10 μM Bis-IV. (M) PMA (1 μM)-mediated increase in mIPSC frequency of an RGC, unaffected by co-application of GLP-1. (N, O) Bar charts summarizing the effects of PMA and GLP-1 on mIPSC frequency (N) and amplitude (O) ($n = 14$). (P) Representative traces of an RGC showing the effect of GLP-1 on mIPSC frequency when 50 μM PKC (19-36) was included in the intracellular solution (PKC_{int}). (Q, R) Bar charts demonstrating the GLP-1-mediated increase in mIPSC frequency (Q), but not amplitude (R) in the presence of PKC_{int} ($n = 11$). Data are presented as mean \pm SEM; ** $P < 0.01$, *** $P < 0.001$, **** $P < 0.0001$, determined by one-way repeated measures analysis of variance with Tukey's multiple comparisons test (B, C, E, F, H, I, K, L, N, O) or paired t -test (Q, R). 2-APB: 2-Aminoethoxydiphenyl borate; BAPTA-AM: 1,2-bis(2-aminophenoxy)ethane-N,N,N',N'-tetraacetic acid tetrakis (acetoxymethyl ester); Bis-IV: bisindolylmaleimide IV; Ctrl: control; GLP-1: glucagon-like peptide-1; IP₃R: inositol trisphosphate receptor; mIPSC: miniature inhibitory postsynaptic current; PI: phosphoinositide; PKC: protein kinase C; PKC (19-36): cell-impermeable PKC inhibitor; PLC: phospholipase C; PMA: phorbol 12-myristate 13-acetate; RGC: retinal ganglion cell; U73122: PI-PLC inhibitor.

Glucagon-like peptide-1 improves diabetes-induced visual dysfunction

Finally, we monitored the effects of GLP-1 eyedrops on visual acuity and contrast sensitivity in early diabetes via measurements of optokinetic response using a virtual optokinetic system (Figure 7A). Average visual acuity was significantly lower in diabetic rats (0.14 ± 0.02 cpd) than in control rats (0.2 ± 0.01 cpd, $P = 0.0258$). Rats treated with GLP-1 maintained a higher level of visual acuity (0.2

± 0.01 cpd) than those treated with PBS (0.16 ± 0.01 cpd, $P = 0.0156$; Figure 7B). Figure 7C shows the contrast sensitivity curves for the different groups, revealing significantly lower contrast sensitivity in the DM group compared with that in the control group ($P = 0.0017$). GLP-1 eyedrops improved contrast sensitivity in diabetic rats, resulting in an upward shift of the curve ($P = 0.0059$ vs. DM + PBS), but did not raise the level to that observed in control rats.



Discussion

In the present study, we have demonstrated the following. (1) The frequency of GABA_AR-mediated mIPSCs was decreased in RGCs of rats subjected to 4 weeks of hyperglycemia. (2) GLP-1 eyedrops enhanced the viability of diabetic RGCs, showing protective effects that were abolished by the GLP-1R antagonist Ex-9-39 or the GABA_AR antagonist SR95531. (3) GLP-1 significantly increased the GABAergic mIPSC frequency in ON- and OFF-RGCs, an enhancement that may be mediated through the GLP-1R/PI-PLC/IP₃R/Ca²⁺/PKC signaling pathway. (4) In diabetic rats, GLP-1 reversed the hyperglycemia-induced increase in spontaneous firing rate and decrease in light-evoked peak firing rate of ON-RGCs, ameliorating the decreases in visual acuity and contrast sensitivity. These findings establish a new mechanism by which activation of GLP-1R modulates functioning of the neuronal GABAergic system via increased inhibitory synaptic input to RGCs, thereby protecting damaged RGCs.

Abnormalities in GABA_AR-mediated neurotransmission are closely related to pathophysiological neurodegenerative disorders. This is the first study to show a reduction in GABAergic mIPSC frequency without alteration of mIPSC amplitude in diabetic ON- and OFF-RGCs, indicating that spontaneous GABA release from ACs to RGCs is decreased in early diabetes (4 weeks). A previous study in diabetic mice showed that, at 6 weeks post streptozocin induction, spontaneous GABA release from ACs to RBCs was increased, while light-evoked GABA release to RBCs was decreased (Moore-Dotson et al., 2016). GLP-1 and GLP-1R have been detected in the inner retinas of rats, mice, and humans (Fan et al., 2014a; Hernández et al., 2016; Hebsgaard et al., 2018), indicating that the GLP-1 system is involved in information processing in the inner retinal circuits. Indeed, our recent study demonstrated that activation of GLP-1R by exendin-4 significantly suppresses L-type Ca²⁺ currents in rat RGCs (Wang et al., 2023). In the present study, we further showed that perfusion of GLP-1 significantly increased the GABAergic mIPSC frequency, but had no effect on amplitude, in both normal and diabetic RGCs. GLP-1 eyedrops also prevented the hyperglycemia-induced decrease in mIPSC frequency. Consistently, exendin-4 was shown to increase the GABAergic mIPSC frequency in gonadotropin-releasing hormone neurons (Farkas et al., 2016) and hypothalamic orexinergic neurons (Acuna-Goycolea and van den Pol, 2004). However, treatment with GLP-1 or GLP-1R agonists did not change mIPSCs in hippocampal CA3 pyramidal neurons (Korol et al., 2015). These results indicate that the modulatory effects of GLP-1 on the inhibitory synaptic transmission vary by cell type.

We observed that GLP-1 significantly enhanced the mIPSC frequency in normal rat RGCs within a specific concentration range (5–100 nM), with no effects at lower or higher concentrations, exhibiting a bell-shaped concentration-response relationship. A similar bell-shaped concentration-response curve was reported in hippocampal CA3 pyramidal neurons (effective concentration range: 0.01–1 nM) (Korol et al., 2015). Notably, we found that diabetic RGCs were more sensitive to GLP-1 than control RGCs, with effective concentrations on mIPSCs ranging from 0.05 to 10 nM. We hypothesize that this difference reflects a compensatory response to the reduction in retinal GLP-1 content caused by hyperglycemia, possibly involving in changes in GLP-1R quantity or sensitivity.

Using pharmacological dissection, we identified the GLP-1R/PI-PLC/IP₃R/Ca²⁺/PKC signaling pathway as a possible mediator of the potentiation effect of GLP-1 on the mIPSCs of RGCs. The GLP-1-mediated increase in mIPSC frequency was abolished by the PI-PLC inhibitor U73122, and was found to be dependent on IP₃R-mediated release of Ca²⁺ from intracellular pools. A previous study showed that IP₃R-mediated Ca²⁺ release also increased GABA release in cultured chicken ACs (Warrier et al., 2005). We further showed that only presynaptic PKC activation was involved in the GLP-1-mediated increase in presynaptic GABA release. A role for the PLC/PKC pathway in the stimulation of insulin secretion has been demonstrated in pancreatic β cells (Shigeto et al., 2017). Activation of presynaptic PKC reportedly increases GABA release in various neurons in the brain (Bartmann et al., 1989; Capogna et al., 1995; Gao and van den Pol, 2000), but the underlying pathway remains unknown. However, PKC regulates exocytotic processes (including neurotransmitter release) in neurons and neuroendocrine cells (Morgan et al., 2005), possibly resulting from phosphorylation of exocytotic proteins associated with vesicle dynamics (Majewski and Iannazzo, 1998; Morgan et al., 2005). Some of these exocytotic proteins, including SNAP-25 and synaptotagmin, are also

present in ACs and their processes (Morgans et al., 1996; Witkovsky et al., 2005; Mesnard et al., 2022). Thus, PKC may increase GABA release in ACs by promoting the phosphorylation of these proteins.

Our study showed that 4 weeks of hyperglycemia led to a marked decrease in RGC density in the peripheral retinal areas, with a less pronounced decline in the central areas. Similar alterations were detected in diabetic (*Ins2^{Akita}*) mice after 3 months of hyperglycemia, in which RGC loss was observed in the peripheral area, but not in the central area (Gastinger et al., 2008). Wang et al. (2023) detected downregulation of GLP-1 mRNA levels in the retinas of 4-week diabetic rats. This work further showed that 2 weeks of treatment with GLP-1 eyedrops promoted RGC survival without altering blood glucose levels in diabetic rats, suggesting a direct protective effect of GLP-1 on RGCs. Although studies have shown that systemic or intraocular administration of GLP-1 or GLP-1R agonists has neuroprotective effects on the retina in diabetic animals, the underlying mechanisms are poorly understood. We demonstrated that the presence of Ex-9-39 or SR95531 blocked the promotional effect of GLP-1 on diabetic RGC survival, suggesting that this GLP-1 action is mediated by GLP-1R and GABA_AR. GABA-modulating drugs have been used clinically as antiepileptic drugs, enhancing inhibitory signals and reducing excitatory signals (Rogawski and Löscher, 2004). Our results also showed that GLP-1 increased GABAergic mIPSC frequency in RGCs. Collectively, these findings suggest that GLP-1 promotes RGC survival by facilitating GABA release from ACs to RGCs in diabetic retinas via activation of GLP-1R, leading to RGC circuit de-excitation and inhibition of excitotoxic processes. The protective mechanisms of GLP-1R activation in the diabetic retina also involve reductions in pro-apoptotic signals, pro-inflammatory cytokines, and extracellular glutamate, increases in pro-survival signals, and an antioxidant effect (Fan et al., 2014b; Hernández et al., 2016; Sampedro et al., 2019; Ramos et al., 2020).

The peak firing rate of an RGC reflects the dynamic range of visual signals that it can process. MEA recordings revealed that 4 weeks of hyperglycemia resulted in a significantly reduced peak firing rate of ON-RGCs, suggesting a decreased dynamic range of processing signals, resulting in altered output to higher visual centers. In contrast, this phenomenon was not observed in OFF-RGCs. Previous studies also showed that the ON signaling pathway in the retina is more susceptible to diabetes. For example, we previously found smaller dendritic fields and altered passive membrane properties in ON-RGA2s (a subtype of ON-RGCs) in 3-month diabetic mice, but not in OFF-RGA2s (a subtype of OFF-RGCs) (Cui et al., 2019). The amplitude of the scotopic electroretinogram b-wave, which reflects the overall activity of RBCs, is reduced in early diabetes in humans and animals (Tzekov and Arden, 1999; Li et al., 2002). Notably, GLP-1 eyedrops significantly increased the peak firing rate of diabetic ON-RGCs, suggesting that GLP-1 enhances the light response in these cells. However, the exact mechanism of this protective effect requires further investigation. The expression levels of GLP-1R in the GCL, inner nuclear layer, and inner plexiform layer (Fan et al., 2014b; Hernández et al., 2016; Cai et al., 2017; Hebsgaard et al., 2018; Shu et al., 2019) suggest that GLP-1 may act directly on RGCs as well as presynaptic ACs. Indeed, our recent study showed that exendin-4 protected diabetic RGCs by inhibiting L-type calcium channels on RGCs (Wang et al., 2023).

In patients and animals with diabetes, decreased visual contrast sensitivity is an early symptom of neuroretinal impairment (Della Sala et al., 1985; Umino and Solessio, 2013; Aung et al., 2014). Although the head tracking response was weaker in our albino rats than in normal rats, we observed visible motion and measurable visual thresholds, which was similar to the results previously obtained in albino rats (Douglas et al., 2005). Our results also showed that diabetic rats exhibited significant decreases in contrast sensitivity and visual acuity. A previous study demonstrated that genetic disruption of the ON signaling pathway reduced the contrast sensitivity of mice, especially at low contrasts (Sarnaik et al., 2014). Therefore, we speculate that the decreased contrast sensitivity in early diabetes may be due to impairment of ON signaling pathway, including the attenuated peak firing rate of ON-RGCs. In addition, because the upper limit of visual acuity in most mammals, including rats, is imposed by the peak density of RGCs (Pettigrew et al., 1988; Gianfranceschi et al., 1999), the decrease in visual acuity induced by hyperglycemia in rats may be related to the decrease in RGC density. We found that GLP-1 eyedrops maintained the visual acuity of diabetic rats at a level similar to that of control animals and partially ameliorated the impairment in contrast sensitivity. This may be attributable, at least in part, to the increases in RGC density and photoresponse induced by GLP-1.

It is important to note that endogenous GLP-1 can be degraded by dipeptidyl peptidase IV (DPP-IV) (Ahrén, 2007). A previous study found DPP-IV mRNA and protein expression in the retinas of diabetic patients and *db/db* diabetic mice, albeit at much lower levels than in the liver or bowel in patients (Hernández et al., 2017). DPP-IV inhibitor-containing eyedrops prevented retinal neurodegeneration in *db/db* mouse retinas by reducing endogenous GLP-1 degradation (Hernández et al., 2017) and/or through other mechanisms (Ramos et al., 2021, 2022). These results suggest the potential usefulness of DPP-IV inhibitor eyedrops.

In summary, our results provide evidence that GLP-1 eyedrops provide neuroprotection in DR, promoting RGC survival by facilitating presynaptic GABA release and increasing visual acuity and contrast sensitivity in diabetic rats. Nevertheless, it is important to acknowledge that this study has some limitations. First, although a previous study showed that the effects of GLP-1R activation were exerted through the cyclic adenosine monophosphate/protein kinase A pathway in pancreatic β cells (Ding and Gromada, 1997), we did not investigate the potential involvement of this pathway in the GLP-1-mediated effect on the mIPSCs of RGCs. Second, the exact mechanism by which topical administration of GLP-1 enhanced the light response of ON-RGCs remains unclear and requires further investigation. Despite these unresolved issues, the findings of this study not only enrich our understanding of the protective mechanisms of GLP-1 in the course of DR, but also provide important clues to guide the eventual transfer of the experimental results to the clinical arena.

Acknowledgments: We would like to thank Dr. Jia-Yi Zhang and Dr. Ru-Yi Yang (Institutes of Brain Science, Fudan University) for their assistance with the optokinetic experiments. Graphical Abstract was created with BioRender.com.

Author contributions: YQS and YMZ designed the experiments. YQS, YCW, LW, HZR, YFL and THZ performed the experiments. YQS, SJW and YMZ analyzed and interpreted the data. YQS, XLY and YMZ wrote the manuscript. All authors read and approved the final manuscript.

Conflicts of interest: The authors declare no competing interests.

Data availability statement: All data relevant to the study are included in the article or uploaded as Additional files.

Open access statement: This is an open access journal, and articles are distributed under the terms of the Creative Commons Attribution-NonCommercial-ShareAlike 4.0 License, which allows others to remix, tweak, and build upon the work non-commercially, as long as appropriate credit is given and the new creations are licensed under the identical terms.

Open peer reviewers: Rafael Simó, Vall d'Hebron Research Institute, Spain; Raj Kumar Pradhan, Thomas Jefferson University, USA.

Additional files:

Additional Figure 1: Changes in blood glucose levels and body weights in diabetic rats.

Additional Figure 2: Characterization of GABA_AR-mediated mIPSCs in rat RGCs.

Additional Figure 3: Eyedrops of GLP-1 could reach the retina without changing the blood glucose levels and body weights of diabetic rats.

Additional Figure 4: Diabetes for 4 weeks did not alter the total retinal area.

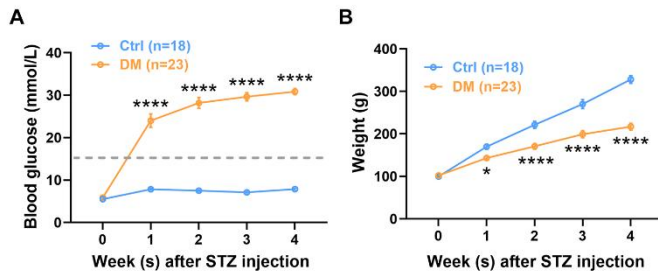
Additional file 1: Open peer review reports 1 and 2.

References

- Acuna-Goycolea C, van den Pol A (2004) Glucagon-like peptide 1 excites hypocretin/orexin neurons by direct and indirect mechanisms: Implications for viscera-mediated arousal. *J Neurosci* 24:8141-8152.
- Ahrén B (2007) GLP-1-based therapy of type 2 diabetes: GLP-1 mimetics and DPP-IV inhibitors. *Curr Diab Rep* 7:340-347.
- Ali SA, Zaitone SA, Dessouki AA, Ali AA (2019) Pregabalin affords retinal neuroprotection in diabetic rats: Suppression of retinal glutamate, microglia cell expression and apoptotic cell death. *Exp Eye Res* 184:78-90.
- Ambati J, Chalam KV, Chawla DK, D'Angio CT, Guillet EG, Rose SJ, Vanderlinde RE, Ambati BK (1997) Elevated gamma-aminobutyric acid, glutamate, and vascular endothelial growth factor levels in the vitreous of patients with proliferative diabetic retinopathy. *Arch Ophthalmol* 115:1161-1166.
- Association for Research in Vision and Ophthalmology (2021) ARVO Statement for the Use of Animals in Ophthalmic and Vision Research.
- Aung MH, Park HN, Han MK, Obertone TS, Abey J, Aseem F, Thule PM, Iuvone PM, Pardue MT (2014) Dopamine deficiency contributes to early visual dysfunction in a rodent model of type 1 diabetes. *J Neurosci* 34:726-736.
- Barber AJ, Baccouche B (2017) Neurodegeneration in diabetic retinopathy: Potential for novel therapies. *Vision Res* 139:82-92.
- Bartmann P, Jackisch R, Hertting G, Allgaier C (1989) A role for protein kinase C in the electrically evoked release of [³H] gamma-aminobutyric acid in rabbit caudate nucleus. *Naunyn Schmiedeberg's Arch Pharmacol* 339:302-305.
- Boni LT, Rando RR (1985) The nature of protein kinase C activation by physically defined phospholipid vesicles and diacylglycerols. *J Biol Chem* 260:10819-10825.
- Cai X, Li J, Wang M, She M, Tang Y, Li J, Li H, Hui H (2017) GLP-1 treatment improves diabetic retinopathy by alleviating autophagy through GLP-1R-ERK1/2-HDAC6 signaling pathway. *Int J Med Sci* 14:1203-1212.
- Capogna M, Gähwiler BH, Thompson SM (1995) Presynaptic enhancement of inhibitory synaptic transmission by protein kinases A and C in the rat hippocampus in vitro. *J Neurosci* 15:1249-1260.
- Carpi-Santos R, Maggessi RS, von Seehausen MP, Calaza KC (2017) Retinal exposure to high glucose condition modifies the GABAergic system: Regulation by nitric oxide. *Exp Eye Res* 162:116-125.
- Charych EI, Liu F, Moss SJ, Brandon NJ (2009) GABA(A) receptors and their associated proteins: implications in the etiology and treatment of schizophrenia and related disorders. *Neuropharmacology* 57:481-495.
- Chen L, Yang XL (2007) Hyperpolarization-activated cation current is involved in modulation of the excitability of rat retinal ganglion cells by dopamine. *Neuroscience* 150:299-308.
- Cui RZ, Wang L, Qiao SN, Wang YC, Wang X, Yuan F, Weng SJ, Yang XL, Zhong YM (2019) ON-type retinal ganglion cells are preferentially affected in STZ-induced diabetic mice. *Invest Ophthalmol Vis Sci* 60:1644-1656.
- Della Sala S, Bertoni G, Somazzi L, Stubbe F, Wilkins AJ (1985) Impaired contrast sensitivity in diabetic patients with and without retinopathy: A new technique for rapid assessment. *Br J Ophthalmol* 69:136-142.
- Ding WG, Gromada J (1997) Protein kinase A-dependent stimulation of exocytosis in mouse pancreatic beta-cells by glucose-dependent insulinotropic polypeptide. *Diabetes* 46:615-621.
- Douglas RM, Alam NM, Silver BD, McGill TJ, Tschetter WW, Prusky GT (2005) Independent visual threshold measurements in the two eyes of freely moving rats and mice using a virtual-reality optokinetic system. *Vis Neurosci* 22:677-684.
- Eggers ED, Carreon TA (2020) The effects of early diabetes on inner retinal neurons. *Vis Neurosci* 37:E006.
- Fan Y, Liu K, Wang Q, Ruan Y, Ye W, Zhang Y (2014a) Exendin-4 alleviates retinal vascular leakage by protecting the blood-retinal barrier and reducing retinal vascular permeability in diabetic Goto-Kakizaki rats. *Exp Eye Res* 127:104-116.
- Fan Y, Liu K, Wang Q, Ruan Y, Zhang Y, Ye W (2014b) Exendin-4 protects retinal cells from early diabetes in Goto-Kakizaki rats by increasing the Bcl-2/Bax and Bcl-xL/Bax ratios and reducing reactive gliosis. *Mol Vis* 20:1557-1568.
- Farkas I, Vastagh C, Farkas E, Bálint F, Skrapits K, Hrabovszky E, Fekete C, Liposits Z (2016) Glucagon-like peptide-1 excites firing and increases GABAergic miniature postsynaptic currents (mPSCs) in gonadotropin-releasing hormone (GnRH) neurons of the male mice via activation of nitric oxide (NO) and suppression of endocannabinoid signaling pathways. *Front Cell Neurosci* 10:214.
- Fritschy JM (2008) Epilepsy, E/I balance and GABA(A) receptor plasticity. *Front Mol Neurosci* 1:5.
- Gao XB, van den Pol AN (2000) GABA release from mouse axonal growth cones. *J Physiol* 523 Pt 3:629-637.
- Gastinger MJ, Kunselman AR, Conboy EE, Bronson SK, Barber AJ (2008) Dendrite remodeling and other abnormalities in the retinal ganglion cells of Ins2 Akita diabetic mice. *Invest Ophthalmol Vis Sci* 49:2635-2642.
- GBD 2021 Diabetes Collaborators (2023) Global, regional, and national burden of diabetes from 1990 to 2021, with projections of prevalence to 2050: a systematic analysis for the Global Burden of Disease Study 2021. *Lancet* 402:203-234.
- Gianfranceschi L, Fiorentini A, Maffei L (1999) Behavioural visual acuity of wild type and bcl2 transgenic mouse. *Vision Res* 39:569-574.
- Göke R, Wagner B, Fehmann HC, Göke B (1993) Glucose-dependency of the insulin stimulatory effect of glucagon-like peptide-1 (7-36) amide on the rat pancreas. *Res Exp Med (Berl)* 193:97-103.
- Hebsgaard JB, Pyke C, Yildirim E, Knudsen LB, Heegaard S, Kvist PH (2018) Glucagon-like peptide-1 receptor expression in the human eye. *Diabetes Obes Metab* 20:2304-2308.
- Hernández C, Bogdanov P, Corraliza L, García-Ramírez M, Solà-Adell C, Arranz JA, Arroba AI, Valverde AM, Simó R (2016) Topical administration of GLP-1 receptor agonists prevents retinal neurodegeneration in experimental diabetes. *Diabetes* 65:172-187.
- Hernández C, Bogdanov P, Solà-Adell C, Sampedro J, Valeri M, Genis X, Simó-Servat O, García-Ramírez M, Simó R (2017) Topical administration of DPP-IV inhibitors prevents retinal neurodegeneration in experimental diabetes. *Diabetologia* 60:2285-2298.
- Honda M, Inoue M, Okada Y, Yamamoto M (1998) Alteration of the GABAergic neuronal system of the retina and superior colliculus in streptozotocin-induced diabetic rat. *Kobe J Med Sci* 44:1-8.

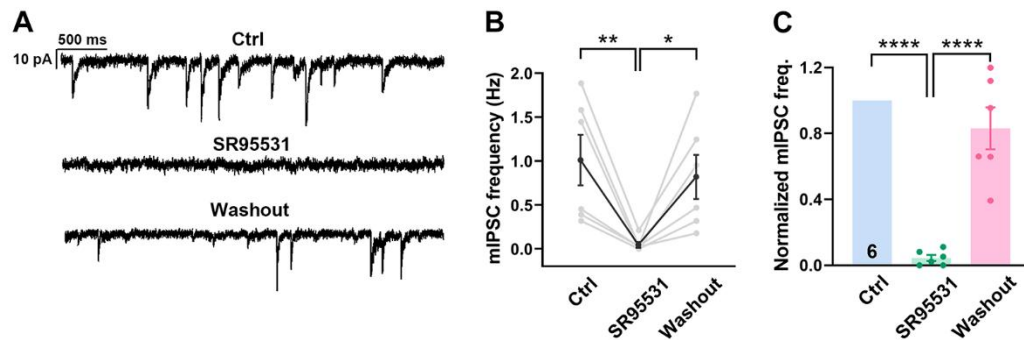
- Ishikawa A, Ishiguro S, Tamai M (1996) Changes in GABA metabolism in streptozotocin-induced diabetic rat retinas. *Curr Eye Res* 15:63-71.
- Juen S, Kieselbach GF (1990) Electrophysiological changes in juvenile diabetics without retinopathy. *Arch Ophthalmol* 108:372-375.
- Kiselyov K, Shin DM, Muallem S (2003) Signalling specificity in GPCR-dependent Ca²⁺ signalling. *Cell Signal* 15:243-253.
- Korol SV, Jin Z, Babateen O, Birnir B (2015) GLP-1 and exendin-4 transiently enhance GABAA receptor-mediated synaptic and tonic currents in rat hippocampal CA3 pyramidal neurons. *Diabetes* 64:79-89.
- Koshal P, Jamwal S, Kumar P (2018) Glucagon-like Peptide-1 (GLP-1) and neurotransmitters signaling in epilepsy: An insight review. *Neuropharmacology* 136:271-279.
- Kowluru RA, Engerman RL, Case GL, Kern TS (2001) Retinal glutamate in diabetes and effect of antioxidants. *Neurochem Int* 38:385-390.
- Layton CJ, Safa R, Osborne NN (2007) Oscillatory potentials and the b-wave: Partial masking and interdependence in dark adaptation and diabetes in the rat. *Graefes Arch Clin Exp Ophthalmol* 245:1335-1345.
- Leasher JL, Bourne RR, Flaxman SR, Jonas JB, Keeffe J, Naidoo K, Pesudovs K, Price H, White RA, Wong TY, Resnikoff S, Taylor HR; Vision Loss Expert Group of the Global Burden of Disease Study (2016) Global estimates on the number of people blind or visually impaired by diabetic retinopathy: a meta-analysis from 1990 to 2010. *Diabetes Care* 39:1643-1649.
- Li Q, Zemel E, Miller B, Perlman I (2002) Early retinal damage in experimental diabetes: electroretinographical and morphological observations. *Exp Eye Res* 74:615-625.
- Liu F, Weng SJ, Yang XL, Zhong YM (2015) Orexin-A potentiates L-type calcium/barium currents in rat retinal ganglion cells. *Neuroscience* 305:225-237.
- Luu CD, Szentlaj JA, Lee SY, Lavanya R, Wong TY (2010) Correlation between retinal oscillatory potentials and retinal vascular caliber in type 2 diabetes. *Invest Ophthalmol Vis Sci* 51:482-486.
- Majewski H, Iannazzo L (1998) Protein kinase C: a physiological mediator of enhanced transmitter output. *Prog Neurobiol* 55:463-475.
- Masland RH (2001) The fundamental plan of the retina. *Nat Neurosci* 4:877-886.
- Masland RH (2012) The neuronal organization of the retina. *Neuron* 76:266-280.
- Mesnard CS, Hays CL, Barta CL, Sladek AL, Grassmeyer JJ, Hinz KK, Quadros RM, Gurumurthy CB, Thoreson WB (2022) Synaptotagmin 1 and 7 in vesicle release from rods of mouse retina. *Exp Eye Res* 225:109279.
- Miya-Coreixas VS, Maggesissi Santos R, Carpi Santos R, Gardino PF, Calaza K (2013) Regulation of GABA content by glucose in the chick retina. *Exp Eye Res* 115:206-215.
- Monnet FP (2005) Sigma-1 receptor as regulator of neuronal intracellular Ca²⁺: Clinical and therapeutic relevance. *Biol Cell* 97:873-883.
- Moore-Dotson JM, Beckman JJ, Mazade RE, Hoon M, Bernstein AS, Romero-Aleshire MJ, Brooks HL, Eggers ED (2016) Early retinal neuronal dysfunction in diabetic mice: Reduced light-evoked inhibition increases rod pathway signaling. *Invest Ophthalmol Vis Sci* 57:1418-1430.
- Morgans CW, Brandstätter JH, Kellerman J, Betz H, Wässle H (1996) A SNARE complex containing syntaxin 3 is present in ribbon synapses of the retina. *J Neurosci* 16:6713-6721.
- Morgan A, Burgoyne RD, Barclay JW, Craig TJ, Prescott GR, Ciuffo LF, Evans GJ, Graham ME (2005) Regulation of exocytosis by protein kinase C. *Biochem Soc Trans* 33:1341-1344.
- Pang JJ, Gao F, Wu SM (2003) Light-evoked excitatory and inhibitory synaptic inputs to ON and OFF alpha ganglion cells in the mouse retina. *J Neurosci* 23:6063-6073.
- Pardue MT, Barnes CS, Kim MK, Aung MH, Amarnath R, Olson DE, Thulé PM (2014) Rodent hyperglycemia-induced inner retinal deficits are mirrored in human diabetes. *Transl Vis Sci Technol* 3:6.
- Pettigrew JD, Dreher B, Hopkins CS, McCall MJ, Brown M (1988) Peak density and distribution of ganglion cells in the retinae of microchiropteran bats: Implications for visual acuity. *Brain Behav Evol* 32:39-56.
- Pulido JE, Pulido JS, Erie JC, Arroyo J, Bertram K, Lu MJ, Shippy SA (2007) A role for excitatory amino acids in diabetic eye disease. *Exp Diabetes Res* 2007:36150.
- Ramos H, Bogdanov P, Sampedro J, Huerta J, Simó R, Hernández C (2020) Beneficial effects of glucagon-like peptide-1 (GLP-1) in diabetes-induced retinal abnormalities: involvement of oxidative stress. *Antioxidants (Basel)* 9:846.
- Ramos H, Bogdanov P, Sabater D, Huerta J, Valeri M, Hernández C, Simó R (2021) Neuromodulation induced by sitagliptin: A new strategy for treating diabetic retinopathy. *Biomedicines* 9:1772.
- Ramos H, Bogdanov P, Huerta J, Deàs-Just A, Hernández C, Simó R (2022) Antioxidant effects of DPP-4 inhibitors in early stages of experimental diabetic retinopathy. *Antioxidants (Basel)* 11:1418.
- Rogawski MA, Löscher W (2004) The neurobiology of antiepileptic drugs. *Nat Rev Neurosci* 5:553-564.
- Ruan HZ, Wang LQ, Yuan F, Weng SJ, Zhong YM (2021) Orexin-A differentially modulates inhibitory and excitatory synaptic transmission in rat inner retina. *Neuropharmacology* 187:108492.
- Salcedo I, Tweedie D, Li Y, Greig NH (2012) Neuroprotective and neurotrophic actions of glucagon-like peptide-1: an emerging opportunity to treat neurodegenerative and cerebrovascular disorders. *Br J Pharmacol* 166:1586-1599.
- Sampedro J, Bogdanov P, Ramos H, Solà-Adell C, Turch M, Valeri M, Simó-Servat O, Lagunas C, Simó R, Hernández C (2019) New insights into the mechanisms of action of topical administration of GLP-1 in an experimental model of diabetic retinopathy. *J Clin Med* 8:339.
- Sarnaik R, Chen H, Liu X, Cang J (2014) Genetic disruption of the On visual pathway affects cortical orientation selectivity and contrast sensitivity in mice. *J Neurophysiol* 111:2276-2286.
- Shigeto M, Cha CY, Rorsman P, Kaku K (2017) A role of PLC/PKC-dependent pathway in GLP-1-stimulated insulin secretion. *J Mol Med (Berl)* 95:361-368.
- Shu X, Zhang Y, Li M, Huang X, Yang Y, Zeng J, Zhao Y, Wang X, Zhang W, Ying Y (2019) Topical ocular administration of the GLP-1 receptor agonist liraglutide arrests hyperphosphorylated tau-triggered diabetic retinal neurodegeneration via activation of GLP-1R/Akt/GSK3 β signaling. *Neuropharmacology* 153:1-12.
- Teo ZL, Tham YC, Yu M, Chee ML, Rim TH, Cheung N, Bikbov MM, Wang YX, Tang Y, Lu Y, Wong IY, Ting DSW, Tan GSW, Jonas JB, Sabanayagam C, Wong TY, Cheng CY (2021) Global prevalence of diabetic retinopathy and projection of burden through 2045: systematic review and meta-analysis. *Ophthalmology* 128:1580-1591.
- Tian N, Copenhagen DR (2003) Visual stimulation is required for refinement of ON and OFF pathways in postnatal retina. *Neuron* 39:85-96.
- Tzekov R, Arden GB (1999) The electroretinogram in diabetic retinopathy. *Surv Ophthalmol* 44:53-60.
- Umino Y, Solesio E (2013) Loss of scotopic contrast sensitivity in the optomotor response of diabetic mice. *Invest Ophthalmol Vis Sci* 54:1536-1543.
- Vilchis C, Salceda R (1996) Effect of diabetes on levels and uptake of putative amino acid neurotransmitters in rat retina and retinal pigment epithelium. *Neurochem Res* 21:1167-1171.
- Wang L, Deng QQ, Wu XH, Yu J, Yang XL, Zhong YM (2013) Upregulation of glutamate-aspartate transporter by glial cell line-derived neurotrophic factor ameliorates cell apoptosis in neural retina in streptozotocin-induced diabetic rats. *CNS Neurosci Ther* 19:945-953.
- Wang YC, Wang L, Shao YQ, Weng SJ, Yang XL, Zhong YM (2023) Exendin-4 promotes retinal ganglion cell survival and function by inhibiting calcium channels in experimental diabetes. *iScience* 26:107680.
- Warrier A, Borges S, Dalcino D, Walters C, Wilson M (2005) Calcium from internal stores triggers GABA release from retinal amacrine cells. *J Neurophysiol* 94:4196-4208.
- Weng S, Wong KY, Berson DM (2009) Circadian modulation of melanopsin-driven light response in rat ganglion-cell photoreceptors. *J Biol Rhythms* 24:391-402.
- Witkovsky P, Arango-Gonzalez B, Haycock JW, Kohler K (2005) Rat retinal dopaminergic neurons: Differential maturation of somatodendritic and axonal compartments. *J Comp Neurol* 481:352-362.
- Yang R, et al. (2023) Assessment of visual function in blind mice and monkeys with subretinally implanted nanowire arrays as artificial photoreceptors. *Nat Biomed Eng* doi: 10.1038/s41551-023-01137-8.
- Zhang XJ, Liu LL, Wu Y, Jiang SX, Zhong YM, Yang XL (2011a) σ receptor 1 is preferentially involved in modulation of N-methyl-D-aspartate receptor-mediated light-evoked excitatory postsynaptic currents in rat retinal ganglion cells. *Neurosignals* 19:110-116.
- Zhang Y, Zhang J, Wang Q, Lei X, Chu Q, Xu GT, Ye W (2011b) Intravitreal injection of exendin-4 analogue protects retinal cells in early diabetic rats. *Invest Ophthalmol Vis Sci* 52:278-285.

P-Reviewers: Simó R, Pradhan RK; C-Editor: Zhao M; S-Editors: Yu J, Li CH; L-Editors: Kahmeyer-Gabbe M, Yu J, Song LP; T-Editor: Jia Y



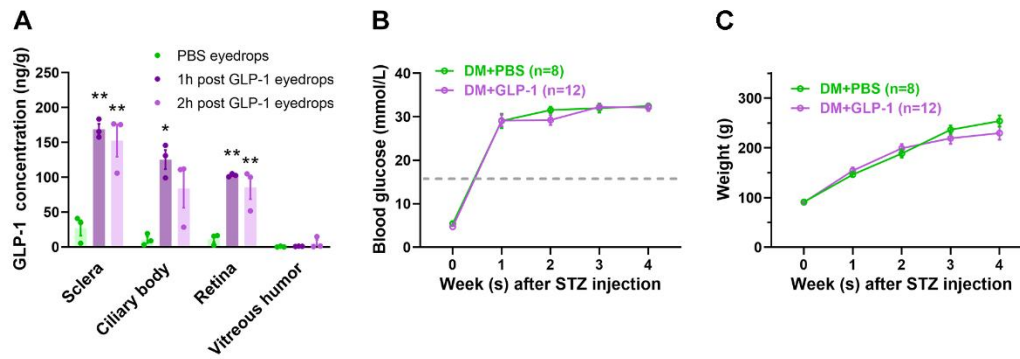
Additional Figure 1: Changes in blood glucose levels and body weights in diabetic rats.

(A) Compared with control rats ($n = 18$), STZ-injected animals ($n = 23$) showed a more than 3-fold increase in blood glucose levels at all four time points. The dashed line in the graph represents a blood glucose value of 16.7 mM. (B) STZ-injected rats gained less body weight than control animals over the course of the study. Data are presented as mean \pm SEM. * $P < 0.05$, **** $P < 0.0001$, two-way analysis of variance with Sidak's multiple comparisons test. Ctrl: control; DM: diabetes mellitus; STZ: streptozocin.



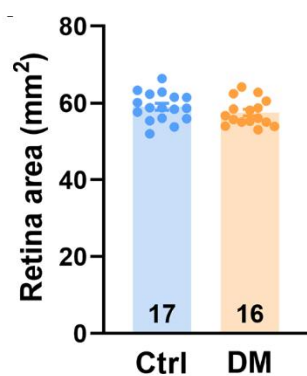
Additional Figure 2: Characterization of GABA_AR-mediated mIPSCs in rat RGCs.

(A) In the presence of D-APV (50 μ M), DNQX (10 μ M), strychnine (10 μ M) and TTX (0.5 μ M) in ACSF and QX-314 (4 mM) in patch pipette, mIPSCs were studied using whole-cell voltage-clamp recording. Representative recordings show that 10 μ M SR95531 completely and reversibly eliminated GABA_AR-mediated mIPSCs of an RGC, recorded at a holding potential of -60 mV. (B, C) Scatterplots of mIPSC frequency from individual recordings (B) and normalized mIPSC frequency (C) demonstrating that the changes of mIPSC frequency after SR95531 application ($n = 6$). Data are presented as mean \pm SEM. * $P < 0.05$, ** $P < 0.01$, **** $P < 0.0001$, one-way repeated measures analysis of variance with Tukey's multiple comparisons test. ACSF: artificial cerebrospinal fluid; Ctrl: control; D-APV: D-2-amino-5-phosphonopentanoic acid; DNQX: 6,7-dinitroquinoxaline-2,3-dione; GABA_AR: γ -aminobutyric acid sub-type A receptor; mIPSC: miniature inhibitory postsynaptic current; RGC: retinal ganglion cell; SR95531: γ -aminobutyric acid sub-type A receptor antagonist; TTX: tetrodotoxin.



Additional Figure 3: GLP-1 eyedrops could reach the retina without changing the blood glucose levels and body weights of diabetic rats.

(A) ELISA assessing GLP-1 levels, showing that GLP-1 levels were significantly increased in sclera, ciliary body and retina ($n = 3$) 1 or 2 hours after GLP-1 administration by eyedrops. $*P < 0.05$, $**P < 0.01$, one-way analysis of variance with Tukey's multiple comparisons test. (B, C) Blood glucose levels (B) and body weights (C) in diabetic rats treated with GLP-1 eyedrops ($n = 12$) were similar to those in diabetic rats treated with eyedrops of PBS ($n = 8$) throughout the study. $P > 0.05$, two-way analysis of variance. Data are presented as mean \pm SEM. DM: diabetes mellitus; ELISA: enzyme-linked immunosorbent assay; GLP-1: glucagon-like peptide-1; PBS: phosphate-buffered saline; STZ: streptozocin.



Additional Figure 4: Diabetes for 4 weeks did not alter the total retinal area.

There was no significant difference in the total retinal area between the control (n = 17) and diabetic (n = 16) groups. Data are presented as mean \pm SEM, and were analyzed by unpaired *t*-test. Ctrl: control; DM: diabetes mellitus.